Signal generation mechanisms, intracavity-gas thermal-diffusivity temperature dependence, and absolute infrared emissivity measurements in a thermal-wave resonant cavity

Jun Shen, Andreas Mandelis,[a] and Helen Tsai
Department of Mechanical and Industrial Engineering, Photothermal and Optoelectronic Diagnostics Laboratories (PODL), University of Toronto, 5 King's College Road, Toronto, Ontario M5S 3G8, Canada

(Received 22 September 1997; accepted for publication 8 October 1997)

The operating thermal power transfer mechanisms in a thermal-wave resonant cavity were explored theoretically and experimentally. Both steady-state ac (thermal-wave) and dc temperature rise were considered, and conduction and radiation heat transfer modes were found to co-exist in the cavity. By introducing controlled variable offset dc resistive heating superposed on the fixed-amplitude thermal-wave oscillation, it was also found that the thermal-diffusivity values of the intracavity gas can vary sensitively as a function of the dc temperature rise within a thin boundary layer adjacent to the cavity thermal source (a metallic Cr–Ni alloy strip). This resulted in the measurement of the temperature dependence of the thermal diffusivity of air. Furthermore, the observed dominance of thermal-wave radiation power transfer in the phase channel of the thermal-wave signal at large cavity lengths allowed the measurement of the absolute infrared emissivity of the thin Cr–Ni strip source material: $\varepsilon = 0.091 \pm 0.004$. © *1998 American Institute of Physics.*
[S0034-6748(98)01501-9]

I. INTRODUCTION

The thermal-wave resonant cavity (TWRC) introduced in this Laboratory[1] has been successfully applied to measure the thermal diffusivities of gases with very high precision and resolution.[2,3] The cavity consists of two parallel walls: one wall is either a laser-heated thin film[1,2] or an electrically resistive thin-film element[3] with an ac current generating a surface heat flux at frequency f; the other wall is a thermal-to-electrical energy transducer, such as a pyroelectric thin film (e.g., polyvinylidene fluoride, PVDF). The transducer produces an ac electrical signal proportional to the energy of the standing thermal-wave pattern-equivalent[1] in the cavity at the position of the transducer. By scanning the cavity length L, one can observe spatially damped resonancelike extrema in both lock-in in-phase and quadrature channels. Assuming that the heat transfer within the cavity is due to purely thermal conduction, i.e., in the absence of convection or radiation, a theory has been advanced for the TWRC.[1,3] which predicts position of the nth extreme $L_n^{(\mathrm{IP})}$ in the in-phase channel as:

$$L_n^{(\mathrm{IP})} = \left(n - \frac{1}{2}\right)\frac{\lambda_g}{2}, \quad n = 1,2,3..., \tag{1a}$$

and the position of the nth extreme $L_n^{(\mathrm{Q})}$ in the quadrature channel as

$$L_n^{(\mathrm{Q})} = \frac{n}{2}\lambda_g, \quad n = 1,2,3,... . \tag{1b}$$

Here,

$$\lambda_g = 2\sqrt{\pi \alpha_g / f} \tag{2}$$

is the thermal-wave wavelength in the intracavity gaseous medium with thermal diffusivity α_g. Therefore, the thermal diffusivity α_g can be deduced by measuring the relative distance of two adjacent extrema, and no signal normalization is needed. α_g can also be extracted by fitting the full theory to the experimental data. The difference of the α_g values obtained by these two methods is within 0.5%.[3]

Although the pure thermal conduction theory[1,3] fits the in-phase and quadrature signals very well, it has been found that it is not consistent with the signal change in the lock-in phase channel with the cavity length L. This indicates that the heat transfer in the cavity may not be purely due to heat conduction, and that other heat transfer mechanisms, such as IR radiation, should be considered. Furthermore, it has been found that the measured thermal diffusivity values increase with increasing voltage across the electrically resistive thin film.[3] This may be the effect of the dc temperature rise in the intracavity gas medium. In this work, a proper analysis of the experimental results is made and a generalized thermal-wave resonant cavity theory is advanced, which takes the thermal radiation and dc temperature rise into account. This theory is found to be in excellent agreement with the experimental data in all lock-in amplifier channels (in-phase, quadrature, amplitude, and phase). In addition, the generalized theory allows the calculation of the otherwise hard-to-measure IR emissivity of the electrically resistive thin-film thermal-wave source.

II. INSTRUMENTATION AND EXPERIMENT

Figure 1 shows the schematic diagram of the TWRC. A Cr–Ni thin-film resistive heating strip with low thermal time constant is used, which carries simultaneous dc and ac currents resulting from the application of appropriate voltages from a signal generator. The Joule-effect heating in the resistive heater produces a dc temperature rise, in addition to

[a]Electronic mail: mandelis@mie.utoronto.ca

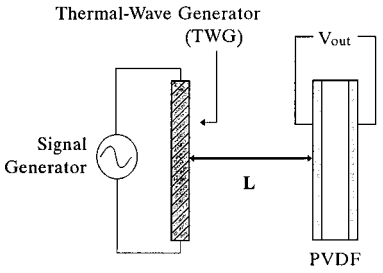

FIG. 1. Schematic diagram of the TWRC.

being the ac thermal-wave source; it is labeled thermal-wave generator (TWG) in Fig. 1. The dc and ac currents generated in the TWG can be controlled by varying the dc offset of the voltage generator's output waveform and the ac voltage across the TWG, respectively. A PVDF circular film, 52-μm-thick and 0.8 cm in diameter, is enclosed in an Inficon® housing and acts as the thermal-wave signal transducer. The pyroelectric signal from the PVDF is then amplified by a preamplifier (ITHACO model 1201), as shown in Fig. 2, and its output is fed into a lock-in amplifier (EG&G model 5204). The TWG is mounted on a micrometer stage, allowing the cavity length to vary as desired automatically by a step motor controlling the micrometer stage with 10-μm resolution. Data acquisition is facilitated with a personal computer connected to the lock-in amplifier through an analog to digital (A/D) converter. The TWRC is placed in an enclosed cell which provides a thermodynamically controlled environment to give equilibrium measurements of the values of thermal diffusivity of the intracavity gas. The gas samples used in this work were air (ultra zero) and helium (99.995%) from Matheson®, Canada. The cavity length was scanned to measure the gas thermal diffusivities at a fixed voltage/current modulation frequency.

In order to investigate the thermal-wave signal mechanisms of the TWRC, three experiments were conducted. To begin with, for air medium the ac voltage amplitude across the TWG was changed from 1.5 to 5.0 V while the dc voltage was kept at 0 V. The dc temperature rises in the TWCR

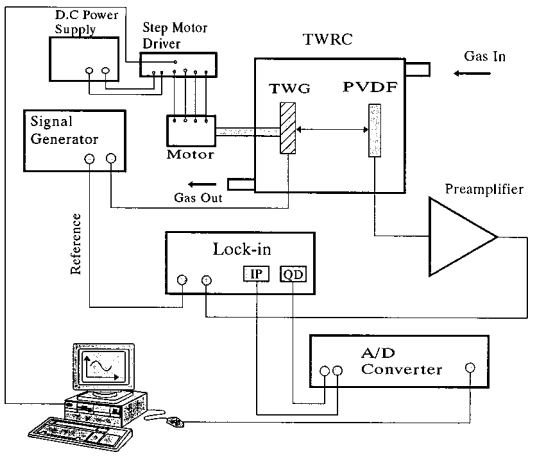

FIG. 2. Block diagram of the experimental system, including the TWG metal-strip heater and the PVDF transducer cavity.

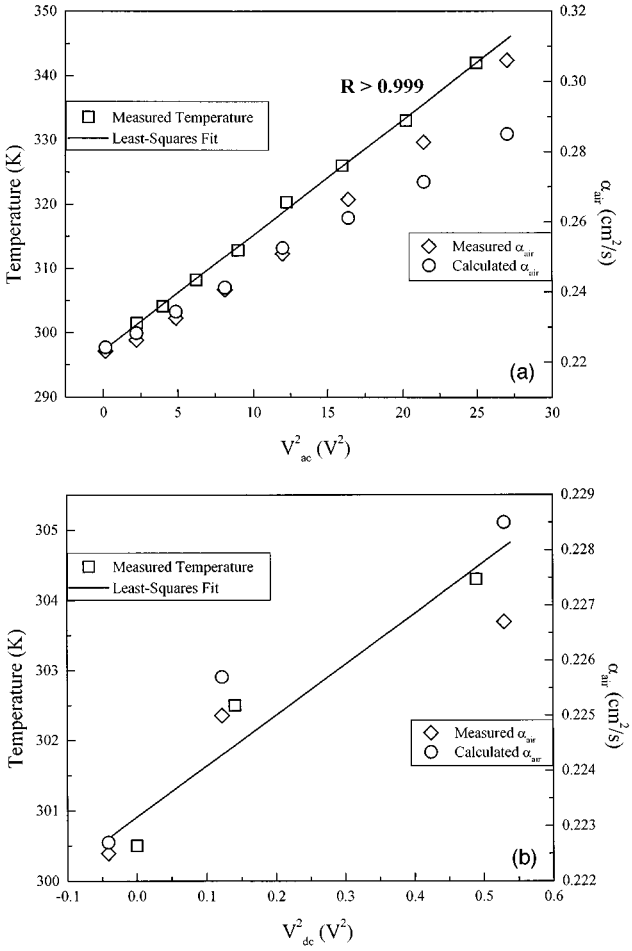

FIG. 3. Variations of dc temperature and thermal diffusivity of intracavity air with voltage changes across the TWG. The calculated thermal diffusivity of air is under the assumption that the thermal diffusivity changes linearly with temperature as 0.0015 cm^2/s K and α_{air}=0.2222 cm^2/s at 300 K.[3,9] (a) ac voltage variation; (b) dc voltage variation.

corresponding to these ac voltage increases were measured by using a glass thermometer contacting the TWG. Then, the ac voltage was kept at 1.457 V and the dc voltage was varied from 20 to 700 mV. The temperature rises due to the dc voltage increases were also measured. The thermal diffusivity of the air corresponding to each voltage change was measured three times and averaged. For helium, an experiment similar to the first experiment in air was conducted, and the ac voltage was changed from 2.0–3.0 V at 0 V dc.

III. RESULTS AND CAVITY THEORY

Figure 3(a) shows the experimental results of the thermal diffusivity measurements corresponding to the first experiment in air. When the ac voltage was varied from 1.5 to 5.0 V, the thermal diffusivity of the air in the intracavity region changed from 0.2231 to 0.3060 cm^2/s as measured by fitting the TWRC theory[3] to the data at each value of the applied voltage (indicated ''measured α_{air}''). The measured dc temperature, T_{wdc}, on the TWG is also displayed in Fig. 3; it was found to be linear in the square of the ac voltage amplitude, V^2_{ac} with correlation coefficient of $R>0.999$. The intercept of the linear least-squares (best) fit to the temperature curve was found to be 297.2 K, in very good agreement with

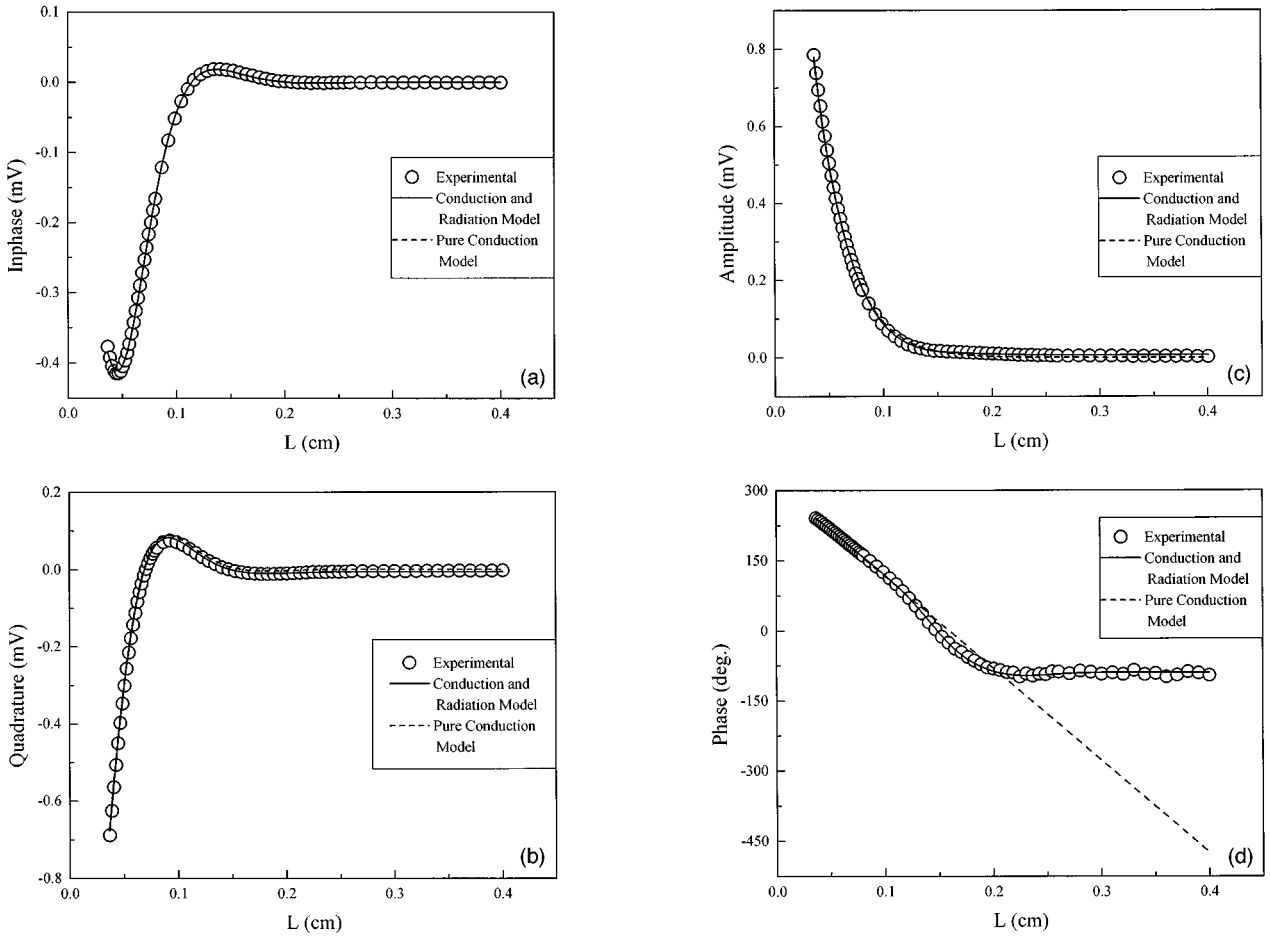

FIG. 4. Experimental and theoretical curves vs the TWRC length L at $f=82.5$ Hz. Sample: air, $V_{ac}=2.0$ V, $V_{dc}=0$ V (a) in-phase; (b) quadrature; (c) amplitude; and (d) phase signal channels.

the simultaneously measured ambient temperature $T_\infty = 297.0 \pm 0.2$ K. Figure 3(b) shows similar results of changing the dc voltage applied across the thin-film heater of the TWG. Overall, Fig. 3 indicates that both ac and dc voltage ramps can change significantly the dc temperature of the TWG, and thus the thermal diffusivity of the intracavity gas, which is a function of the dc temperature of the TWG. Consequently, to be able to explain these phenomena, the dc temperature rise of the TWG must be included in a complete theoretical model for the TWRC. Even though the three lock-in amplifier signal channels, in-phase, Fig. 4(a), quadrature, Fig. 4(b) and amplitude, Fig. 4(c) show good-to-excellent agreement with the purely conductive theory,[3] the phase channel, Fig. 4(d), deviates significantly from the straight-line behavior predicted by that theory and appears relatively flat when the cavity length is greater than ca. 200 μm. In what follows, all the possible intracavity heat transfer mechanisms (convection, conduction, and thermal radiation) will be considered in a generalized TWRC model.

A. Convection

Regarding convection in the TWRC, the intracavity space is assumed to contain quiescent gas, with no occurrence of heat transfer due to forced convection. To justify this assumption, the extent of the importance of natural convection in the heat transfer mechanism in the TWRC can be assessed by the Grashof number, a dimensionless parameter:[4]

$$Gr = \frac{gB\Delta TL^3}{\nu^2}, \tag{3}$$

where g is the acceleration due to gravity; B is the coefficient of thermal expansion for the intracavity gas, ($B=1/T$ for ideal gases, where T is the gas temperature); ΔT and L are the temperature difference and distance between the two walls of the TWRC, respectively; and ν is the viscosity of the gas. The Grashof number represents the ratio of the buoyancy forces to the viscous force in natural convection. For the enclosure between two parallel plates, natural convection is unimportant for Grashof number below 2000.[4] Here, the gas temperature T can be replaced by $T_\infty = 297.2$ K. ΔT can be evaluated as the difference between the maximum dc temperature of the TWG and the ambient temperature, which was <60 K during the course of these experiments. The maximum distance between the two walls of the cavity is <4 mm. The viscosities ν for air and helium at 300 K are[5] 1.589×10^{-3} and 1.22 cm^2/s, respectively. The Grashof numbers for air and helium are thus calculated to be 500 and 3.2, respectively. Seeing that $Gr \ll 2000$ in both cases, it can be concluded that natural convection is negligible.

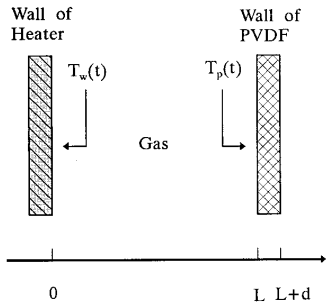

FIG. 5. Configuration diagram of the TWRC for the one-dimensional heat transfer model.

B. Conduction and radiation

To consider thermal conduction and radiation in the TWRC, one-dimensional heat conduction equations are used. Referring to the one-dimensional geometry of Fig. 5, valid for wide and long thin-film heaters compared to the length of the cavity, as in the case of the present configuration, the following boundary value problem for the TWRC[6] is pertinent

$$\frac{\partial^2 T_g(x,t)}{\partial x^2}-\frac{1}{\alpha_g}\frac{\partial T_g(x,t)}{\partial t}=0; \quad 0\leqslant x\leqslant L, \tag{4a}$$

$$\frac{\partial^2 T_p(x,t)}{\partial x^2}-\frac{1}{\alpha_p}\frac{\partial T_p(x,t)}{\partial t}=0; \quad L\leqslant x. \tag{4b}$$

α_j and k_j ($j=g$ and p, refers to gas and PVDF) are the thermal diffusivity and conductivity of medium j, respectively. Boundary conditions for Eqs. (4a) and (4b) are

$$T_g(0,t)=T_w(t), \tag{5a}$$

$$T_g(L,t)=T_p(L,t), \tag{5b}$$

and, assuming direct radiation heat transfer from the heater to the surface of the wide spectra bandwidth PVDF transducer, followed by absorption and thermal conversion of the radiated power:

$$-k_p\frac{\partial T_p(x,t)}{\partial x}\bigg|_{x=L}+k_g\frac{\partial T_g(x,t)}{\partial x}\bigg|_{x=L} =\sigma\epsilon[T_w^4(t)-T_p^4(L,t)]. \tag{5c}$$

Here $\sigma=5.6697\times10^{-12}$ W cm^{-2} K^{-4} is the Stefan–Boltzmann constant; $\epsilon(0\leqslant\epsilon\leqslant1)$ is the IR emissivity of the TWG. The right-hand side of Eq. (5c) is the *net* rate of radiant heat exchange between the TWG and PVDF surface at $x=L$. In Eq. (5),

$$T_w(t)=\frac{1}{2}T_a(1+e^{i\omega t})+T_d+T_\infty \tag{6}$$

is the temperature of the TWG wall/source. It consists of dc and ac components, $T_{\rm wdc}$ and $T_{\rm wac}$:

$$T_w(t)=T_{\rm wdc}+T_{\rm wac}e^{i\omega t}, \tag{6'}$$

where $T_{\rm wdc}=\frac{1}{2}T_a+T_d+T_\infty$ and $T_{\rm wac}=\frac{1}{2}T_a$. T_a is the amplitude of ac temperature component; T_∞ is, as before, the ambient temperature of the medium surrounding the cavity; T_d is one of the dc temperature components, the result of the application of a dc voltage across the TWG. When $T_{\rm wac}$ is much smaller than $T_{\rm wdc}$,

$$T_w^4(t)\approx T_{\rm wdc}^4+4T_{\rm wdc}^3T_{\rm wac}e^{i\omega t}. \tag{7a}$$

Similarly,

$$T_p^4(L,t)\approx T_{\rm pdc}^4(L)+4T_{\rm pdc}^3(L)T_{\rm pac}(L)e^{i\omega t}, \tag{7b}$$

if $T_{\rm pac}(L)\ll T_{\rm pdc}(L)$. Here $T_{\rm pdc}(L)$ and $T_{\rm pac}(L)$ are dc and ac temperature components, respectively, at the surface of the PVDF transducer ($x=L$). Therefore, $T_w^4(t)-T_p^4(L,t)$ in Eq. (5c) can be approximated by

$$T_w^4(t)-T_p^4(L,t)\approx[T_{\rm wdc}^4-T_{\rm pdc}^4(L)]+4[T_{\rm wdc}^3T_{\rm wac}-T_{\rm pdc}^3(L)T_{\rm pac}(L)]e^{i\omega t}. \tag{8}$$

The solutions to Eqs. (4a) and (4b) can be expressed as

$$T_g(x,t)=\psi_1(x)e^{i\omega t}+\psi_2(x), \tag{9a}$$

$$T_p(x,t)=\phi_1(x)e^{i\omega t}+\phi_2(x). \tag{9b}$$

Here ω is the angular modulation frequency ($\omega=2\pi f$). $\psi_1(x)$ and $\phi_1(x)$ are the ac temperature fields, and $\psi_2(x)$ and $\phi_2(x)$ the dc components.

1. dc solutions

The steady-state solutions to the partial differential Eqs. (4a) and (4b) can be written as

$$\psi_2(x)=Ax+B; \quad 0\leqslant x\leqslant L, \tag{10a}$$

$$\phi_2(x)=C(x-L)+D; \quad L\leqslant x. \tag{10b}$$

A, B, C, and D are constants which can be determined by the boundary conditions, Eqs. (5a)–(5c) and by the additional inhomogeneous boundary condition

$$\phi_2(L+d)=T_\infty, \tag{11}$$

here d is the thickness of the PVDF. To simplify the solution by transforming Eq. (11) to a homogeneous boundary condition, let

$$T_{\rm pdc}(L)=T_\infty+\Delta T, \tag{12a}$$

under the reasonable assumption:

$$\Delta T\ll T_\infty. \tag{12b}$$

$T_{\rm pdc}^4$ can then be expressed as

$$T_{\rm pdc}^4(L)\approx T_\infty^4\left(1+4\frac{\Delta T}{T_\infty}\right)=4T_\infty^3T_{\rm pdc}(L)-3T_\infty^4. \tag{13}$$

The boundary condition, Eq. (5c), for the dc solution becomes

$$-k_p\frac{\partial T_p(x,t)}{\partial x}\bigg|_{x=L}+k_g\frac{\partial T_g(x,t)}{\partial x}\bigg|_{x=L} =\sigma\epsilon[T_{\rm wdc}^4+3T_\infty^4-4T_\infty^3T_{\rm pdc}(L)]. \tag{14}$$

The integration constants in Eqs. (10a) and (10b) can thus be determined

$$A=\frac{\sigma\epsilon d(T_{\mathrm{wdc}}^4+3T_\infty^4-4T_\infty^3T_{\mathrm{wdc}})+k_p(T_\infty-T_{\mathrm{wdc}})}{k_gd+k_pL+4\sigma\epsilon dLT_\infty^3}, \tag{15a}$$

$$B=T_{\mathrm{wdc}}, \tag{15b}$$

$$C=\frac{k_g(T_\infty-T_{\mathrm{wdc}})+\sigma\epsilon L(T_\infty^4-T_{\mathrm{wdc}}^4)}{k_gd+k_pL+4\sigma\epsilon dLT_\infty^3}, \tag{15c}$$

$$D=T_{\mathrm{pdc}}(L)=\frac{\sigma\epsilon dL(3T_\infty^4+T_{\mathrm{wdc}}^4)+k_pLT_\infty+k_gdT_{\mathrm{wdc}}}{k_gd+k_pL+4\sigma\epsilon dLT_\infty^3}. \tag{15d}$$

2. ac solutions

The ac components, $\psi_1(x)$ and $\phi_1(x)$, can be expressed as[7,8]

$$\psi_1(x)=Ee^{-\sigma_gx}+Fe^{\sigma_gx}, \quad 0\leqslant x\leqslant L, \tag{16}$$

$$\phi_1(x)=Ge^{-\sigma_p(x-L)}, \quad L\leqslant x. \tag{17}$$

Here,

$$\sigma_j\equiv(1+i)\sqrt{\frac{\pi f}{\alpha_j}}; \tag{18}$$

E, F, and G are constants to be determined by the boundary conditions Eqs. (5) and (8). For the purposes of solving the ac boundary value problem, the PVDF transducer is considered to be totally thermally thick,[7] i.e., semi-infinite on the scale of the spatially damped thermal wave in the PVDF. Furthermore, only the integration constant G is of practical importance, as it alone determines the transducer response, which is related to the measurable signal output. After some algebraic manipulations one obtains

$$G=\frac{T_a\left\{2b_{gp}\exp(-\sigma_gL)+\dfrac{H}{k_p\sigma_p}[1-\exp(-2\sigma_gL)]\right\}}{(1+b_{gp})-\left(1-b_{gp}+\dfrac{4\sigma\epsilon}{k_p\sigma_p}T_{\mathrm{pdc}}^3(L)\right)\exp(-2\sigma_gL)}, \tag{19}$$

where

$$H\equiv4\sigma\epsilon T_{\mathrm{wdc}}^3, \tag{20}$$

$$b_{gp}\equiv\frac{k_g\sqrt{\alpha_p}}{k_p\sqrt{\alpha_g}}. \tag{21}$$

For the thermally thick ($\sigma_pd\gg1$) PVDF film of small thermal time constant, $\omega\tau_{\mathrm{th}}\ll1$ the pyroelectric (PE) voltage response is[8]

$$V(f)=S(f)\frac{G}{\sigma_p}, \tag{22}$$

where $S(f)$ is an instrumental factor, a constant for a fixed modulation frequency. The pyroelectric voltage $V(f)$ is the average of the thermal-wave field over the transducer thickness and can be expressed using Eq. (19):

$$V(f,L)=\frac{T_a\dfrac{S(f)}{\sigma_p}\left\{2b_{gp}\exp(-\sigma_gL)+\dfrac{H}{k_p\sigma_p}[1-\exp(-2\sigma_gL)]\right\}}{(1+b_{gp})-\left(1-b_{gp}+\dfrac{4\sigma\epsilon}{k_p\sigma_p}D^3\right)\exp(-2\sigma_gL)}. \tag{23}$$

The real part of Eq. (23), Re$[V(f,L)]$, stands for the demodulated signal in the lock-in amplifier in-phase (IP) channel; the imaginary part, Im$[V(f,L)]$, corresponds to the signal in the quadrature (Q) channel.

Compared with the purely heat conduction cavity theory,[3]

$$V(f,L)=\frac{2T_aS(f)b_{gp}\sigma_p^{-1}\exp(-\sigma_gL)}{(1+b_{gp})-(1-b_{gp})\exp(-2\sigma_gL)}, \tag{24}$$

Eq. (23) contains additional $\sigma\epsilon$-dependent terms in both numerator and denominator, resulting from the contributions of thermal radiation. The $\sigma\epsilon$-dependent term, $4\sigma\epsilon D^3/(k_p\sigma_p)$, in the denominator of Eq. (23) is much smaller than 1. Recalling that D is equal to the dc temperature at the cavity ''wall'' (the surface of the PE transducer), if $D=400$ K and $f=70$ Hz, this term is about 10^{-3}. Therefore, Eq. (23) can be simplified

$$V(f,L)=\frac{T_a\dfrac{S(f)}{\sigma_p}\left\{2b_{gp}\exp(-\sigma_gL)+\dfrac{H}{k_p\sigma_p}[1-\exp(-2\sigma_gL)]\right\}}{(1+b_{gp})-(1-b_{gp})\exp(-2\sigma_gL)}. \tag{23'}$$

The radiation (H-dependent) term in the numerator of Eqs. (23) or (23′) affects both the IP and the Q signal channels, especially when L is large, although the H term is small. Figure 4 shows that the generalized theory, Eq. (23′), gives excellent fits to the experimental data. Both the purely conductive cavity theory, Eq. (24), and the present one, Eq. (23′), fit the IP data equally well because their real parts are essentially the same, and the resonance condition, Eq. (1a), is valid for both. The intracavity gas thermal diffusivity can be measured by determining the relative distance between adjacent extreme, e.g., $n=1$ and 2 in Eq. (1a), in the IP signal. There is a slight difference between the Q-channels of the two theories, Fig. 4(b), especially when L is large, due to the radiation term in Eq. (23′). The position of the extreme is, nevertheless, the same for both theories in Fig. 4(b). Similarly, both theories predict almost the same behavior for the amplitude channel as shown in Fig. 4(c), with a slightly higher contribution to the signal from the present theory at large values of L, due to the presence of the radiation-dependent term. The most pronounced difference, however, between the two theories occurs in the phase channel, Fig. 4(d). Unlike the straight line phase-lag behavior predicted by the purely conductive mechanism, when thermal radiation is taken into account the phase saturates beyond a certain cavity length, as the thermal-wave power ''centroid'' becomes dominated by the radiant heat transfer across the cavity. This model is in excellent agreement with the experimental data, indicating that thermal radiation does play a significant role in the heat transfer mechanism of the TWRC, especially when L is large, and that the signal phase is the appropriate channel to observe and measure this mechanism.

Radiation heat transfer, however, is not so important in the dc temperature spatial profile as a function of the cavity length L. In Eq. (15a), upon setting $\epsilon=1$, $T_\infty=297.2$ K, $d=52$ μm, $T_{\mathrm{wdc}}=350$ K, when L changes from 0 to 4 mm the term $4\sigma\epsilon dLT_\infty$ in the denominator is 2×10^{-3} times smaller than the sum, $k_g d+k_p L$, and the $\sigma\epsilon d(T_{\mathrm{wdc}}^4+3T_\infty^3-4T_\infty^3T_{\mathrm{wdc}})$ term in the numerator is 10^{-4} times smaller than $k_p(T_\infty-T_{\mathrm{wdc}})$.

The average dc temperature of the intracavity gas is

$$\langle T_g\rangle=\frac{1}{L}\int_0^L(Ax+B)dx=\frac{1}{2}AL+B. \tag{25}$$

Figure 6 shows how the average temperature, $\langle T_g\rangle$, of intracavity air varies with L; this is not a straight line because A, Eq. (15a), is a function of L. Figure 6 also shows that the amplitude of the thermal-wave signal decays steeply with increasing L, in accordance with the expected (photo)pyroelectric theoretical behavior,[7] indicating that sizable thermal-wave (ac) signals can only be obtained at the position of the transducer when L is small and commensurate with the thermal diffusion length in the gas. The average dc temperature $\langle T_g\rangle$ of the intracavity gas attenuates even faster than the thermal-wave spatial profile. Figure 6 shows that only a very thin boundary layer of gas adjacent to the TWG has significant dc temperature rise. As discussed earlier in this section, Figs. 3(a) and 3(b) show an increase in the measured thermal diffusivity value of air with increasing TWG dc temperature. The measured values are comparable to the calculated values

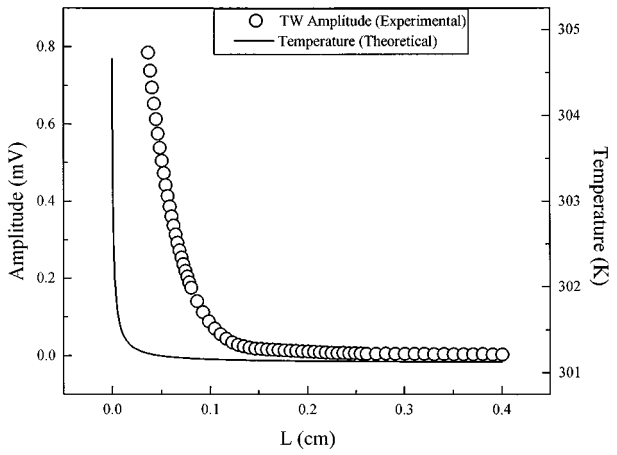

FIG. 6. Experimental thermal-wave signal amplitude and theoretical average dc temperature $\langle T_g\rangle$ of the intracavity air vs the TWRC length L. $\epsilon=1$; $T_\infty=297.2$ K; $d=52$ μm; $k_p=1.3\times10^{-3}$ cm^2/s,[7] $k_g=2.62\times10^{-4}$ cm^2/s,[9] $T_{\mathrm{wdc}}=305$ K. Other conditions are the same as in Fig. 4.

obtained by use of the measured TWG dc temperature and the assumption that α_{air} changes linearly with temperature at the rate of 0.0015 cm^2/s K in the range of 300–350 K.[9] Good agreement between the values of α_{air} obtained by the two independent measurement methods was found (''measured'', and ''calculated'' α_{air} data points in Fig. 3). It can thus be concluded that the thin thermal boundary layer in the TWRC plays the key role in determining the thermal diffusivity value of the intracavity gas. Similar conclusions were reached by Bertolotti *et al.*[10] in their investigation of the temperature profile in fixed-length and scanned-length TWRCs with the temperature profile probed by the photothermal beam deflection technique.

IV. IR EMISSIVITY MEASUREMENTS

The fact that radiation heat transfer affects the cavity-length-scanned signal profile, especially the phase channel, Fig. 4(d), provides a convenient method to measure the IR emissivity of the TWG thin-film heater. The absolute value of this physical parameter is otherwise difficult to determine for arbitrary thin-layered materials. Parameters, such as T_a and α_g, in Eq. (23′), can be found by fitting Eq. (23′) to the IP channel data. The values of H, Eq. (20), corresponding to the various V_{ac} amplitude and V_{dc} values in these experiments can be determined by fitting Eq. (23′) as a single-parameter equation to the experimental data of the phase signals. Since the dc temperature T_{wdc} is linear in both V_{ac}^2 and V_{dc}^2, for both experimental cases in Figs. 3(a) and 3(b), it can be expressed as the superposition

$$T_{\mathrm{wdc}}=T_\infty+C_1V_{\mathrm{dc}}^2+C_2V_{\mathrm{ac}}^2, \tag{26}$$

where, C_1 and C_2 are constants to be determined. By using Eq. (20), H can be written as

$$H=4\sigma\epsilon(T_\infty+C_1V_{\mathrm{dc}}^2+C_2V_{\mathrm{ac}}^2)^3. \tag{27}$$

The absolute value of emissivity ϵ of the TWG can be determined by fitting Eq. (27) to the values of H obtained from the theoretical fit to the phase, Fig. 4(d). Figure 7 shows one

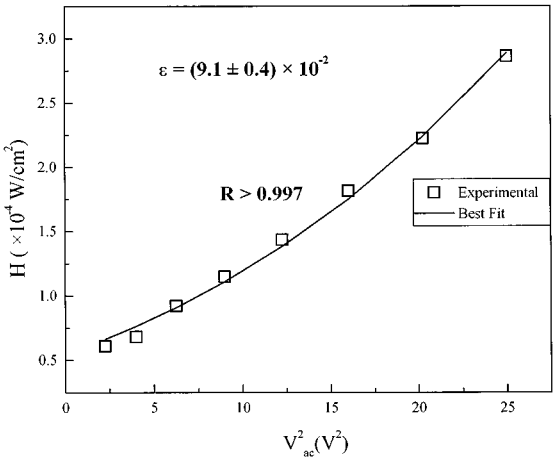

FIG. 7. Radiation heat transfer coefficient H vs. V_{ac}^2. The absolute value of $\epsilon=(9.1\pm0.4)\times10^{-2}$ was found by fitting Eq. (27) to the experimental data.

of the fits associated with the $V_{dc}=0$ experiment in air. The IR emissivity of the TWG heater strip Cr–N material was then found to be $\epsilon=0.091\pm0.004$ with a correlation coefficient $R>0.997$. In the air experiments with $V_{dc}>0$, $\epsilon=0.088$ was found. Although in the these latter experiments the V_{dc} was changed only three times, resulting in a not very precise ϵ value, the difference between the two foregoing ϵ values is only about 3.2%. From visual inspection it could be seen that the color of the resistive film of the TWG was gray, which renders this emissivity value quite reasonable. This experimental methodology can be extended to measure the absolute value of IR emissivity of other thin layered materials, by use of the remote laser-beam modulated heating technique introduced in Ref. 1.

These measurements were also repeated in a helium atmosphere, however, the ϵ value thus measured was much smaller. Compared with air, helium has much higher thermal conductivity and thermal diffusivity, and the intracavity temperature rises, both ac and dc, with the same voltages applied across the TWG are much greater. Therefore, the theoretical linearization assumption, Eq. (12b), is not likely to be satisfied, which would inevitably complicate the quantitative analysis and invalidate the present methodology, if gases with high thermal conductivity and diffusivity, such as helium are used for absolute ϵ measurements.

V. DISCUSSION

A complete theoretical and experimental thermal-wave signal generation analysis of the TWRC has been undertaken. It was found that, in addition to the thermal conduction, thermal radiation plays an important role in the heat transfer process at large cavity lengths compared to the thermal diffusion length. The theory is in excellent agreement with experimental data of in-phase, quadrature, amplitude, and phase signals. On taking into consideration the dc component of the thermal distribution profile in the cavity, in combination with the thermal-wave phase sensitivity to the radiation heat transfer coefficient, a method was developed which allowed the reliable measurement of the absolute value of the IR emissivity, $\epsilon=(9.1\pm0.4)\times10^{-2}$, of the thin-film heating strip material (Cr–Ni), an otherwise difficult to determine parameter.

ACKNOWLEDGMENTS

The support of the Materials and Manufacturing Ontario (MMO) and of Imperial Oil, Sarnia, ON, is gratefully acknowledged.

[1] J. Shen and A. Mandelis, Rev. Sci. Instrum. **66**, 4999 (1995).
[2] J. Shen, A. Mandelis, and D. Aloysius, Int. J. Thermophys. **17**, 1241 (1996).
[3] J. Shen, A. Mandelis, and T. Ashe, Int. J. Thermophys. (in press).
[4] G. C. M. Meijer and A. W. Herwaarden, *Thermal Sensors* (Institute of Physics, Bristol and Philadelphia, 1994).
[5] F. P. Incropera and D. P. Dewitt, *Fundamental Heat and Mass Transfer*, 3rd ed. (Wiley, New York, 1990).
[6] H. S. Carslaw and J. C. Jaeger, *Conduction of Heat in Solids*, 2nd ed. (Oxford, London, 1959).
[7] A. Mandelis and M. M. Zver, J. Appl. Phys. **57**, 4421 (1985).
[8] A. Mandelis, J. Vanniasinkam, S. Budhudu, A. Othonos, and M. Kokta, Phys. Rev. B **48**, 6808 (1993).
[9] J. P. Holman, *Heat Transfer*, 7th ed. (McGraw-Hill, New York, 1990).
[10] M. Bertolotti, G. L. Liakhou, R. Li Voti, S. Paoloni, and C. Sibilia, Int. J. Thermophys. (in press).